

## Chapter 10

# Jets and Outflows

The ejection of prodigious amounts of material during birth still puzzles us. It is paradoxical that just when we expect to observe infall, the signatures of outflow prevail. Ultimately, we want to know why. Are we witnessing simply the disposal of waste material – the placenta being cast aside? Or are outflows essential, a means of removing some ingredient which allows the rest to flow inwards? There are reasons to believe it is the latter, in which case outflows hold the key to the formation of individual stars.

Outflows may also determine the destiny of entire clusters of stars. They remove gravitational energy from a small scale and feed it back into the large-scale cloud. Done at high speed, the cloud is disrupted and dispersed. The outflow feedback thus influences the star formation efficiency. The young cluster stars are then subject to less gravitational pull and, consequently, also disperse into looser associations and, eventually, the general field.

All protostars and all young stars with accretion disks appear to drive powerful outflows of some kind. Outflows are driven by accretion. If we can understand how the outflow evolves as the accretion proceeds, we can perhaps understand how the star evolves. First, we need to investigate from where this material originates and the launching mechanism in operation. Progress has so far proven slow because the structure of each outflow is different: the determining factors are as much environmental as genetic. A variety of spectacular displays have been uncovered over the last twenty years and the common factors and causes are still not established.

Outflows were at first thought to be of no great consequence to star formation and of restricted influence on their environment. They were thought to be merely outbursts lasting ten thousand years during the million-year evolution. This changed with the discovery of gigantic old outflows and the

realisation that the early protostellar stages are also short term. Together, these facts suggested that many outflows maintain a record of events over the entire protostellar history as well as providing an account of present activity.

## 10.1 Classical Bipolar Outflows

In the 1980s, outflows of molecular gas were discovered around many of the youngest stars in star formation regions. Originally, these were mainly associated with high mass stars. The outflows were found to be split into two lobes, one on each side of the young stellar object. Most significantly, the material on one side was found to be predominantly blue shifted and on the opposite side red shifted. This, in itself, does not require the gas to be part of an outflow but other factors leave no other option open. For example, the radial speeds implied by the line shifts are often of the order of tens of  $\text{km s}^{-1}$  on scales larger than 0.1 pc. Such speeds can only be realistically produced from quite near the protostar. Other characteristics, in particular proper motions and jets, have confirmed that these are really outflows.

These bipolar outflows had remained hidden to us until we had developed the technology to observe cold molecular gas. They are best observed in emission lines from the CO molecule at millimetre wavelengths. Employing different transitions and isotopes, we gain information about the temperature, opacity and density, as discussed in §2.3.2. Now, we employ a wide range of molecular tracers and techniques.

Such analyses may give clues to the entire history of the protostar, provided we learn how to decipher what we observe. We can search for signs that the outflow was stronger or more collimated when the driving protostar was younger. If an outflow lobe which now has a linear size of 1 pc has grown at the speed of  $10 \text{ km s}^{-1}$ , then it must be  $10^5$  years old, comparable to the age of a Class I protostar. In general, outflow sizes range from under 0.1 pc to several parsecs. Furthermore, outflow speeds range from a few  $\text{km s}^{-1}$  up to about  $100 \text{ km s}^{-1}$ . Therefore, kinematic ages take on a wide range of values. It should be clear, however, that the kinematic age may not represent the true age.

Also, the total mass in the outflow covers a wide range, from  $10^{-2} M_{\odot}$  to  $10^3 M_{\odot}$ . The mass set in motion, especially in the youngest and most powerful outflows, far exceeds the mass accreted onto the protostar. There-

fore, while processes near the protostar drive a bipolar outflow, it does not provide the material. In other words, we observe material which has been swept-up or entrained.

Even before we could map the features, it was long known that only a small fraction of a lobe produces the molecular emission. The structure within the bipolar lobes can now be resolved, e.g. in HH 211 (Fig. 10.1). We detect thin shells, further indicating that material has been swept up and compressed. Shell or limb structure implies that there is a cavity from which molecular material has been largely evacuated. In other cases, the emission is from numerous clumps spread more evenly. These clumps could be a consequence of fragmentation of the shell.

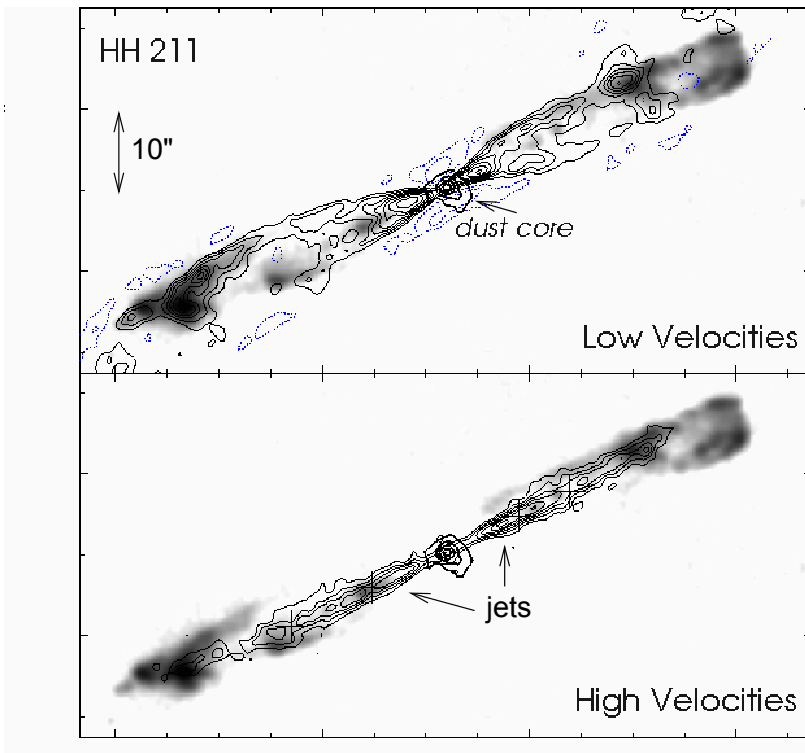


Fig. 10.1 The HH 211 outflow in CO rotational emission (contours) split into two radial velocity components (top panel displays only speeds within  $8 \text{ km s}^{-1}$  of the maternal cloud). The  $\text{H}_2$  near-infrared emission (greyscale) shows the warm shocked gas. (Credit: F. Gueth & S. Guilloteau, *Astron. Astrophys.* 343, 571-584 (1999).)

There are possibly two distinct types of bipolar outflow. The ‘classical’ outflows, which dominated those found in the 1980s, are weakly collimated: wide relaxed-looking structures. The collimation factor,  $q_{coll}$ , defined as the ratio of the lengths of the major to minor axes, is used to distinguish the type of outflow. Classical outflows possess values  $q_{coll} < 4$ . Of course, we view just the projection onto the plane of the sky and projection could cause a highly collimated outflow, orientated close to the line of sight, to appear very wide. However, there is no equivalent sample of highly collimated outflows to suggest that the low collimation is purely an effect of projection. Classical bipolar outflows have quite low kinematic ages, in the range  $2\text{--}5 \times 10^4$  yr. In contrast, outflow statistics suggest an outflow duration of  $2 \times 10^5$  yr.

Quadrupolar outflows possess two red and two blue shifted lobes. Their arrangement is consistent with an interpretation as two independent superimposed bipolar outflows. There are several examples, including Cepheus E and L 273. Multiple young stars are found near the centroids of these lobes. In fact multiple sources are often found through deep radio or near-infrared observations. Therefore, it appears that if each source undergoes an outflow phase, then the phase cannot last for the total star formation period.

A major goal is to determine how the momentum, however ejected, is transferred to the ambient medium. Combined spatial and radial velocity distributions of the gas contain information on how the gas is accelerated. The radial velocity data of numerous outflows display a pattern referred to as a ‘Hubble Law’. That is, the maximum velocity increases roughly linearly with distance from the outflow source. We also find that higher speeds are observed closer to the outflow axis. Two interpretations have been advanced: we may be observing the expansion of one or more bow-shaped shells with the overall lobe shape being preserved during the expansion. Or, material is ejected with a range of speeds and directions during outbursts, directly into the observed pattern.

The high thrusts of the outflows pose a serious problem for their origin (see §10.8.2). The transfer of momentum from a stellar wind would have to be very efficient. A high efficiency of momentum transfer could be obtained if the flow were energy driven. This requires a means to transfer the energy into the ambient medium instead of the momentum. This is not easy to accomplish except in a spherical expansion within which the accelerated gas remains hot. The observed flows, however, do not possess large inflated bubbles or predicted high lateral motions. Instead, bipolar outflows often display strong forward-directed motion.

## 10.2 High-collimation Bipolar Outflows

During the 1990s, a new class of bipolar outflow was revealed. These outflows are distinguished by their high collimation with  $q_{coll}$  occasionally exceeding 20. The measured collimation depends on the observed radial velocity: the highest collimation is found when we restrict the data to just the highest velocity gas.

There is a continuity between the classical and the high-collimation outflows. The many common features include shell structures, Hubble laws, and kinematic ages. In addition, the new outflows possess gas moving with extremely high velocities (EHV). What makes the speeds, exceeding  $50 \text{ km s}^{-1}$ , in some sense extreme is that we would expect molecules to be destroyed during the acceleration process if a shock wave were responsible. Sometimes, the EHV component is contained within compact clumps, hence termed ‘bullets’. In the L 1448 outflow from a Class 0 protostar, the bullets are symmetrically placed about the driving protostar.

Of great significance to the star formation story is that the outflows with high collimation are mainly driven by Class 0 protostars whereas the classical outflows are driven mainly by Class I protostars. Furthermore, the highly collimated flows are more energetic than classical outflows when compared to the protostellar luminosity. It is thus apparent that the outflow power is strongly dependent on the accretion rate. Outflows are usually characterised by the momentum flow rate rather than the power since this quantity, the thrust, can usually be more accurately measured. In terms of evolution, there is evidence that outflows become less collimated as the protostar evolves.

Spectroscopic differences are also found. The main diagnostics are those of CO line profiles which are interpreted in terms of the fraction of mass accelerated to high speeds. The high-collimation flows tend to have relatively high mass fractions at high speeds while more evolved outflows, as well as the more massive outflows, tend to contain lower fractions of high speed gas. The obvious interpretation is that the injection of high-speed gas decreases and the reservoirs of slow-moving gas accumulate as an outflow ages. The data are however rather fragmentary and various effects are difficult to separate.

Analysis of the radial velocity also indicates that the gas is in ‘forward motion’ in the higher collimated outflows. That is, there is very little motion transverse to the axis. This indicates that the sweeping is not through simple snowploughing since a plough would deflect material sideways. In-

stead, the momentum delivered from the source is efficiently transferred. On the other hand, classical bipolar outflows often display overlapping blue and red lobes and multiple components, consistent with their wide opening angles. Overlapping outflow lobes have also been very commonly associated with X-ray emitting protostars. This suggests the existence of thick obscuring disks with a rotation axis orientated close to the line of sight. In such pole-on configurations, the X-rays escape through the outflow cavity.

The significance of the disk in directing the outflow is now well established. The outflow axes are often directed transverse to circumstellar disks where resolved. HH 211 is an excellent example of this (see Fig. 10.1 & 9.1).

### 10.3 Molecular Jets

Jets are now believed to be present in all young stellar objects in which infall is taking place. The word ‘jets’ is rather a loose term for all slender structures which appear to emanate from close to a young star and have the appearance of being high speed directed flows.

Jets from Class 0 protostars are found to be extremely powerful, dense and molecular. The structures are usually observed in the near-infrared through their emission in lines of molecular hydrogen. Hence, surveys for near-infrared jets are now an important means of detecting new Class 0 protostars. Long before an outflow has accumulated a detectable amount of cool CO gas, and before the protostar is detectable in the near-infrared or visible wave bands, the birth is already heralded by molecular jets. The lines are produced when the molecules are vibrationally agitated, requiring shock waves of at least  $10 \text{ km s}^{-1}$  to be present. With improving sensitivity, jets are now also being found in tracers of cooler molecular gas such as CO and SiO. It is also possible to detect cool atomic gas from some jets in the near-infrared but, in general, we would not expect to detect any optical jets due to the obscuration by surrounding dust.

Although there are examples of twin jets, molecular and atomic jets are usually found emanating from just one side of the source (see Fig. 10.2). Nevertheless, there are indications for the existence of a second jet in many of these outflows. Quite often, we are unable to detect either of the purported jets possibly due to the extinction. In such cases, we can attempt to disentangle a jet component from the region of impact where the jet is brought to a halt (§10.5). The jets rarely contain any smooth diffuse structure but more often consist of a chain of arc-shaped aligned clumps

separated on scales of between 1000 AU and 10,000 AU. The clumps of emission are called ‘knots’ and are often bow shaped. Symmetrically located knots in twin-jet sources indicate that the knots originate from centrally-generated disturbances. These pulsations steepen up into shocks as they propagate along the jet. Within the pulses, compressed jet material accumulates to form dense cold bullets as detected in CO rotational lines. As the pulses move out along the jet, the strengths of the shocks decay and all the material is swept into the bullets. In this manner, a continuous jet is transformed into a chain of knots.

In the vicinity of the dust-enshrouded central stars, jets can still be found at radio wavelengths. The emission on scales under 100 AU testifies to the presence of aligned ionised gas jets, producing radiation through the free-free mechanism. In the radio, we can pinpoint the location of the source. With present continental-wide radio telescope networks such as the Very Long Baseline Array (VLBA), we can attain an angular resolution down to sub-milliarcseconds, which corresponds to sub-AU scale spatial scales in nearby star-forming regions. H<sub>2</sub>O maser emission at 22.235 GHz is frequently detected in low-mass YSOs and is known to be a good tracer of jet activity very close to protostars while other masers are associated with protostellar disks. The masers are highly time variable on timescales of a day to a month. The maser luminosities correlate well with the luminosities of the radio continuum emission, also suggesting that masers trace the jet activity. They both appear to be excited in the shocked layer between the ambient protostellar core and jet.

Jets from Class I protostars are generally fainter. On large scales, these jets can often be detected in the optical emission lines. The main tracers are the H $\alpha$  and [S II] lines (Fig. 10.3), which indicate that the jets are of low excitation typically produced behind shocks of speed 20–140 km s<sup>-1</sup>. Molecular emission is often also observed coincident with the major optical atomic knots within the jets.

Several molecular jets display an almost linear increase in fluid speed with distance. Jet speeds inferred from proper motions of knots and radial speeds are generally quite low, between 40–100 km s<sup>-1</sup>, in Class 0 jets. However, in the HH 111 jet, speeds above 200 km s<sup>-1</sup> are found from both atomic and molecular components.

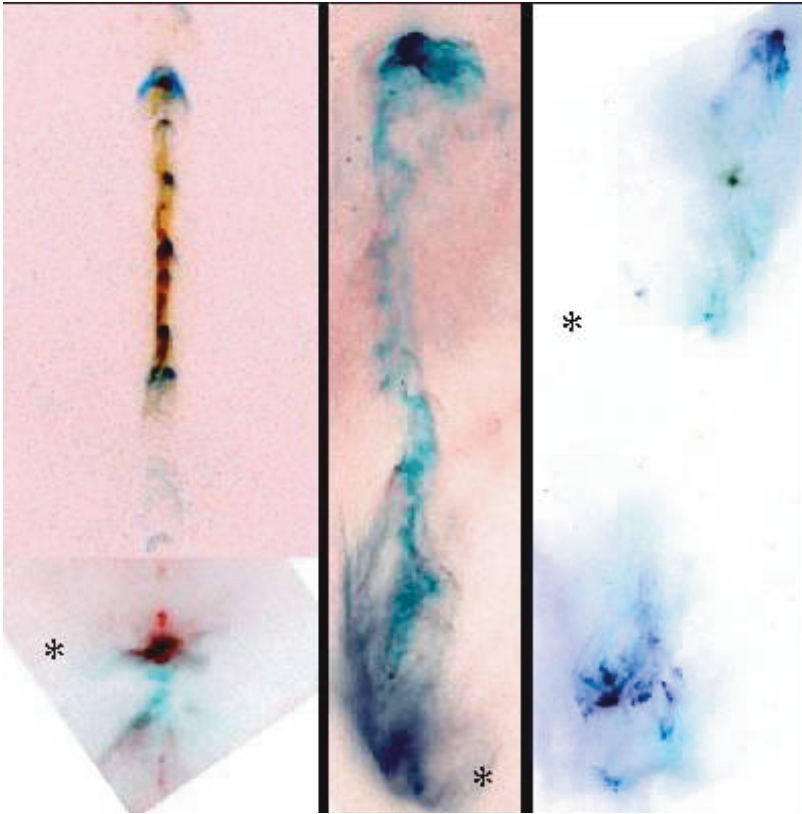


Fig. 10.2 The various optical manifestations of outflows driven by jets in atomic gas. The left panel displays the inner regions of the bright and knotty HH 111 (driving stars are indicated by an asterisk adjacent to their location). The middle panel displays HH 47, driven from a young star within the diffuse reflection nebula. A turbulent jet leads to a wide bow shock. Both these outflows possess counter-jets moving away from us (into the cloud) and, hence, show up better in near-infrared observations. The right panel displays the pair of HH Objects HH 1 (top) and HH 2 (bottom) driven by an obscured star close to the centre (not the visible star closer to the top). (Credit: NASA, HST & HH 111: B. Reipurth (CASA/U. Colorado) *et al.*, HH 47: J. Morse, NASA, HST. HH 1/2: J. Hester (ASU))

#### 10.4 Atomic Jets

The jets from Class II sources are almost exclusively atomic. Molecular signatures have disappeared. The line fluxes arise from within 1000 AU. After careful subtraction of the stellar continuum, microjet structure on scales under 100 AU can be revealed. In about 30% of the Class II sources,

microjets are indeed found. These are short highly collimated optical jets with knots that display proper motions of a few hundred  $\text{km s}^{-1}$ .

Although these jets are weak and the accretion has subsided, the jets have attracted attention because they are observable at visible wavelengths. The Hubble Space Telescope (HST) and large telescopes with adaptive optics have given us glimpses of the structure on sub-arcsecond scales (§9.1). Through these observations, we hope to learn about the jet launching mechanism. Many strands of evidence have been uncovered from jets in the Taurus region, such as the following:

- The collimation occurs on scales large compared to the radius of the young star. Jets are only weakly collimated on the scale of  $\sim 50$  AU whereas the stellar radius is  $\sim 0.02$  AU.
- The jets are focused to within an angle of  $\sim 10^\circ$  after 1000 AU.
- The jets are knotty with the knots typically displaying proper motion of 100–200  $\text{km s}^{-1}$ .
- The line profiles are broad and blue shifted to 100–400  $\text{km s}^{-1}$ . The lower velocity is located around the edges and displays signs of acceleration with distance from the source.
- Jet speed tends to increase with the stellar luminosity.
- Variations in the jet speed are quite common.
- Asymmetries are observed in the radial velocity between the jet and counterjet.

In addition, the HST has helped to uncover irradiated jets where an external UV radiation field contributes to the excitation and visibility. These jets are produced by visible low-mass young stars in the immediate vicinity of OB stars. The young stars appear to have lost their parent cloud cores. The jets are either one-sided or with the brighter jet pointing away from the irradiating star and about an order of magnitude brighter than the counterjet. Spectroscopy shows that the fainter counterjets are moving several times faster than the main jets. Thus the brightness asymmetry reflects an underlying kinematic asymmetry. Furthermore, some of the Orion Nebula jets power chains of knots and bow shocks that can be traced out to 0.1 pc from their sources.

## 10.5 Herbig-Haro Flows

Besides the jets, a series of bow-shaped structures occur on larger scales. These extend out to several parsecs, forming the ‘parsec-scale flows’. The apices of the bows face away from the protostar, giving the impression that they are being driven out (e.g. Fig. 10.3). Furthermore, proper motions are measured over timespans of a few years which demonstrate that the bow structure as a whole moves away from the source. In the reference frame of the bow, knots of emission move along the bow structure away from the apex into the flanks.

Such objects were first discovered on optical plates in the 1950s, and so obtained their name from their finders: Herbig-Haro (HH) objects. It soon became clear that the emission was excited by the particle collisions expected in shock waves. With higher sensitivity, we now often find complex structures which may extend back to the source. These are called Herbig-Haro flows. We also find outflow activity much further away from the source which suggest kinematic ages of around 30,000 years. Although this is still shorter than the Class I phase, it can be that the outflow direction has varied, so that the advancing edge we now observe has a much shorter kinematic age than the full duration of the outflow.

Models for HH objects as curved shock waves successfully reproduce the observed features. One identifying spectroscopic feature often found is the double-peaked line profile, signifying that the flanks of a bow shock deflect material both away and toward the observer. A problem encountered had been that the bow speed predicted by the spectrum is much lower than observed in the proper motion and radial velocity. How can the shock propagate rapidly without producing high excitation in the atoms? The only plausible answer was that the bow is advancing through material which has already a substantial motion away from the source. That is, many bows that we observe are not driven directly into the ambient cloud but are moving through the outflow itself. This implied that outflows were larger and older than previously imagined and that, if we looked hard and wide, we would find evidence for more distant HH objects. The discovery of these gigantic outflows was made possible by further developments in our instrumentation: we have developed detectors with the capability to image extremely wide fields, up to ten arcminutes wide.

Given the strong evidence that Herbig-Haro objects are bow shocks, they provide stringent tests for our understanding of shock physics and molecular dynamics. Some bows have been imaged in both molecular and

atomic lines. It is then found that the molecular emission arises from the flanks of the bow, whereas the optical atomic emission originates from close to the apex. This separation is expected since the molecules do not survive the high temperatures near the apex. However, given bow speeds which typically exceed  $80 \text{ km s}^{-1}$ , the molecules should only survive in the far wings where the shock component has dropped below  $24 \text{ km s}^{-1}$ . In this case, the shock behaves hydrodynamically with two zones: a jump in temperature and density followed by a long cooling zone (J-shock). In a J-shock, essentially all the heating of the molecules occurs within a narrow zone, a few collisional mean-free-paths wide. Instead, we often measure  $\text{H}_2$  emission from near the bow front. This factor and the low excitation of the molecules suggest that the shock surprise is being cushioned: ambipolar diffusion is softening the shock, spreading the front over a wide cool region which can be resolved. In this way, we gain the opportunity to understand how ambipolar diffusion operates within these C-shocks (where C stands for continuous).

If jets drive bipolar outflows, then we could expect to observe intense radiation from where the supersonic flow impacts against the external gas. While the external shock may correspond to a roughly paraboloidal bow, the jet is expected to be terminated by a round disk-shaped shock, which in fluid dynamics is called a Mach disk. Alternatively, if the impact is within the outflow itself then the interaction creates an ‘internal working surface’. In this case, the two shocks are called a reflected shock and a transmitted shock. They sandwich a growing layer of outflowing gas accumulated through both shocks. In some outflows including HH 34, slower bow shocks are found at larger distances from the driving source, thus displaying an apparent deceleration. This suggests that the bow shocks lose momentum progressively when they drift into the external medium, once they are not directly driven by the jet.

The process by which large quantities of material are swept into the outflow is still not absolutely clear. Most evidence is in favour of a mechanism dubbed prompt entrainment in which the outflowing gas is swept into the wakes of extended bow shocks. The wings and wakes of the bows disturb the ambient material while travelling both within the outflow and advancing directly into the ambient cloud. Recent high resolution  $\text{H}_2$  and millimetre interferometric observations provide supporting evidence. Alternatively, a wide slow stellar wind which surrounds the narrow fast jet would efficiently transfer momentum into the ambient medium. In addition, ambient core material may be entrained into the outflow across a turbulent

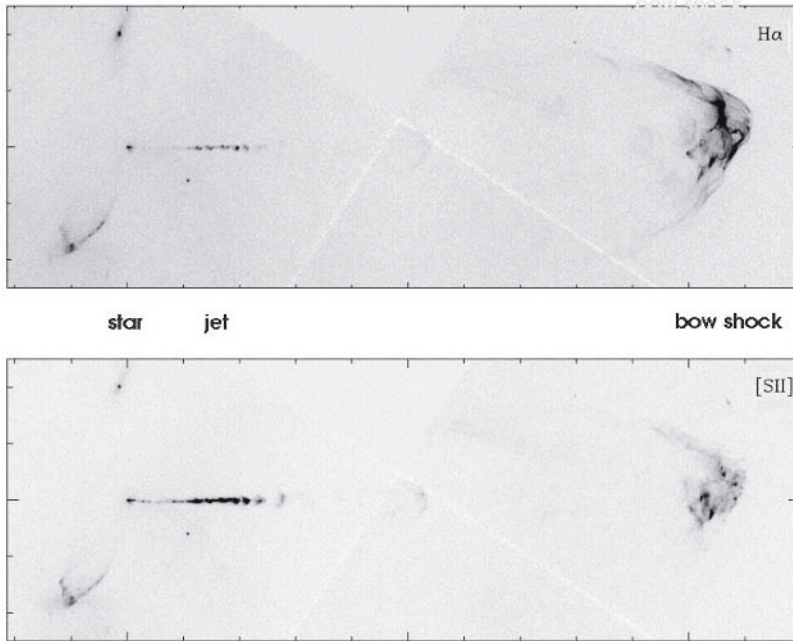


Fig. 10.3 The HH 34 jet and bow shock in two atomic emission lines. The bow shock is strong in the hydrogen tracer of warmer gas (top), while the jet only needs weak shock heating to appear in the sulphur line (bottom). (Credit: B. Reipurth *et al.*, AJ, 123, 362.)

boundary layer. The material is then gradually accelerated and mixed into the outflow.

## 10.6 Launch Theory

A scenario in which infalling gas can be partly ejected and partly accreted is desired. For this reason, understanding outflows may go a long way to determining how stars are made.

Three relevant classes of jet launching model appear in the literature. These are based on how the driving fuel is transferred into supersonic motion. The proposed driving forces are radiation, hydrodynamic and magnetic. The first two classes are usually dismissed on several grounds, especially since they are not all-purpose. Firstly, radiation pressure from the central young star lacks sufficient momentum to drive the molecular out-

flow. Photon momenta are roughly two orders of magnitude too low. Even in the high luminosity sources where most fuelling momentum,  $L_{bol}/c$ , is available, outflows cannot be driven. This could in principle be compensated for by multiple scattering of the photons (tens of times) within the outflow. Such an arrangement is not practical.

Hydrodynamic models can also be sub-divided into at least three types. The classical mechanism for smoothly accelerating a subsonic flow into a supersonic flow has been carried over from the theory of fluid dynamics. This involves a pressure gradient and a well-designed nozzle, called a de Laval nozzle. The astrofluid interpretation is the ‘twin-exhaust’ model in which two nozzles are located along the axis of least resistance. The nozzle shape and locations are determined by the pressure distribution in the protostellar core. The problems with this mechanism are that we do not possess the ambient pressure to contain the subsonic flow nor the solid nozzles which would resist break up as the fluid negotiates the transonic constrictions (i.e. the Kelvin-Helmholtz instability, §10.7). Alternatively, if we relax the requirement for a steady jet, we can obtain a high nozzle pressure by considering a rapidly expanding central cavity, replacing the ambient pressure by ram pressure and so construct expanding de Laval nozzles.

In the candle flame scenario, a central wind is deflected towards the disk rotation axis by an oblique shock surface. After deflection, the shocked fluid is cooled and compressed into a thin supersonic sheath which rams out of the core. In an elaboration on this theme, the central wind is more concentrated along the axis and a toroidal gas core is assumed. The resulting configuration generates wide bow-shaped shells which reproduce the shapes of classical bipolar outflows. These scenarios, besides not directly accounting for jets, do not produce bow shocks with the observed configurations.

In magnetohydrodynamic models, both the wind origin and collimation are accounted for. There are three potential launching sites: the disk, the disk-star interaction zone, and the stellar surface.

The disk wind model involves the gradual collimation of a centrifugally-driven wind from a magnetised accretion disk. The wind energy is derived from the gravitational energy released from the disk. This is accomplished via the gas rotation and a coupled magnetic field. The magnetic field lines behave like rigid wires, spun around as the disk rotates, and ejected packets of material behave like beads threaded on these wires. The crucial factor is the geometry of the magnetic field. If the magnetic field were aligned with the rotation axis, then angular momentum is transferred into the ambient

gas through the propagation of torsional Alfvén waves and the disk is very gradually braked as already described in §7.6. On the other hand, if the field lines thread through the disk but are then bent by more than  $30^\circ$  from the spin axis, then the solid-body co-rotation throws out and accelerates disk material along the field lines. A nice feature of this model is that a small fraction of the accreting material is ejected, carrying with it a large fraction of the angular momentum. In other words, a disk wind permits accretion without the need for an anomalous viscosity as in standard disk theory (see §9.4.2). The main problem is to maintain the strongly bent magnetic field: an hourglass geometry representing squeezed field lines is required to preside after the core and disk contraction although the field lines have a natural tendency to straighten.

The MHD models for launching are complex and predictions difficult to extract. We can summarise some results here based on robust physical concepts. The angular momentum is carried by the rotation of the fluid and the twisted magnetic field. For a streamline originating from the disk at a radius  $R_o$  (i.e. the footpoint), the rotation like a solid body with angular speed  $\Omega_o$  persists out to the Alfvén radius  $R_a$  where the radial speed of the escaping material has reached its Alfvén speed. Hence, within  $R_a$  Alfvén waves can propagate back towards the footpoints. Therefore, this distance corresponds to the lever arm which supplies a back torque onto the disk. The extracted specific angular momentum is  $\Omega_o R_a^2$  and the terminal speed of a cold wind is

$$v_{wind} = 2^{1/2} \Omega_o R_a. \quad (10.1)$$

That is, the terminal wind speed is larger than the disk rotation speed by somewhat more than the ratio of the lever arm to the footpoint radius, which is estimated to be  $R_r/R_o \sim 3$ . To drive the accretion, the required mass outflow is

$$\dot{M}_{wind} \sim \left( \frac{R_o}{R_a} \right)^2 \dot{M}_{acc}. \quad (10.2)$$

Then, all the angular momentum of the disk is removed through the wind while removing  $\sim 10\%$  of the disk mass.

Collimation is achieved through hoop stresses. At the Alfvén radius, the azimuthal field and poloidal field components are equal. Beyond this point, the azimuthal field becomes dominant and the Lorentz force bends the fluid towards the axis. The stability of the resulting jet is assisted by the jet's poloidal field which acts as a spinal column. Note also that the

wind may be launched from a wide surface area of the disk and so the jet may thus display a strong shear with high speeds associated with the spine.

The alternative MHD model is called the X-wind model. As shown in Fig. 10.4, the wind is generated in the zone which connects the stellar magnetosphere to the inner region of a truncated conducting disk. This model, therefore, assumes that the disk does not extend to the protostar during the stages when jets are being produced. The inner disk, located where the disk co-rotates with the protostar or young star, provides the lever arm for launching the jets.

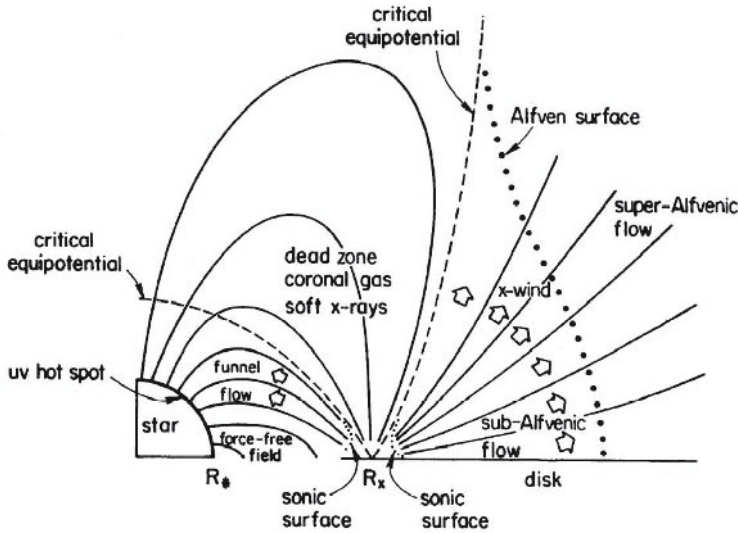


Fig. 10.4 The X-wind model for Classical T Tauri star environments – see text (Credit: F. Shu *et al.* 1994, *Astrophysical J.*, 429,781).

Shielding currents prevent the threading of the disk by magnetospheric field lines. Therefore, the stellar magnetic field originating from the polar regions has to squeeze through the inner hole in the disk and is strongly compressed in the equatorial plane. With some magnetic diffusivity and in the presence of accretion, the field will manage to penetrate the innermost ring of the disk. This field threaded ring is termed the X-region.

The star has to adjust to the angular velocity of the inner disk edge in order to prevent a winding up of the field lines. Material in the innermost part of the X-region rotates at sub-Keplerian velocities (see §9.4.2) and is thus ready to move further in. The magnetic field channels this material

in an accretion funnel towards regions close to the stellar poles, consistent with accretion theory (§9.4.3).

As the gas falls in, it would spin up due to angular momentum conservation if it were free. It is, however, attached to the rigidly rotating field lines and thus exerts a forward torque on the star and, more importantly, on the disk. The angular momentum of the accreting gas is thus stored in the X-region of the disk, which would be spun up. At the same time, the field lines threading the outer part of the X-region are inclined to the disk plane by only a very small angle (they have been squeezed through the disk in the equatorial plane from large distances). Hence, this part of the disk, rotating at super-Keplerian velocities, can launch a magneto-centrifugally driven disk wind: the X-wind. It is powerful enough to open the initially closed stellar field lines (which trace the weak field of the outermost parts of the stellar dipole), allowing the wind to expand. The result is that the X-wind efficiently removes angular momentum from the X-region which has been deposited there by the accretion flow.

The density as well as the velocity of the X-wind increase strongly but smoothly towards the polar axis. In the X-wind picture, the well collimated jets seen as Herbig-Haro or infrared jets are only the densest axial parts of a more extensive structure. The molecular outflow driven by the X-wind may thus be regarded as a hybrid of a jet driven outflow and a cavity swept out by a wide angle wind. In conclusion, the X-wind model is able to account for many observations in one fairly self-consistent model. The observations include time variable accretion/wind phenomena in T Tauri stars, the slow rotation rates of T Tauri stars, protostellar X-ray activity, and a number of the properties of jets and molecular outflows.

Jet launching mechanisms suggest that jets are not waste channels but important spin outlets. Without jets to remove the angular momentum, it is not clear what would then stop the young stars from reaching break-up speeds. Attempts are now being made to confirm that jets rotate. The measurements are difficult since angular momentum conservation predicts that the rotation speed falls as the jet expands. Therefore, the jet axial speed (and variations in it) tends to dominate the identifiable spectral features.

## 10.7 Jet Theory

We explore here the many reasons why jets are not smooth straight structures. The origin of the jet knots has been a subject of great debate. One

initial idea was derived from laboratory experiments where gas jets of high pressure are known to expand and then converge on being injected from a nozzle. This produces oblique crossing shocks and, for specific geometries, the oblique shocks are intercepted by stronger transverse Mach disks on the axis. The result is the appearance of fixed shocks, which could be observable as a pattern of knots with a spacing of a few jet radii. Such a stationary pattern of knots has not as yet been found. In contrast, jet knots move at high speed (see §10.3 & 10.4).

A second knot production scenario which does produce moving knots is analogous to the mechanism which generates ocean waves. An interface between two moving fluids or gases is subject to the Kelvin-Helmholtz instability. The cause is the centrifugal force created when material slides over small corrugations on both sides of the interface. The effect is that small disturbances grow exponentially while they are advected down the jet. The advection speed is low when the jet is lighter than the surroundings which suggests that the instability may be significant in the Class II atomic jets rather than the heavy Class 0 molecular jets.

In terms of possible jet geometries – cylindrical or narrow cones – the instability produces coherent patterns involving pinching modes and helical modes. The penetration and bow shock formation are limited since the jet disintegrates once large-scale modes have developed. This is expected to disrupt a hydrodynamic jet on a length scale of 10–20  $M_j R_j$  where  $M_j = v_j/c_j$  is the Mach number of the jet of radius  $R_j$ . On the other hand, other effects such as certain magnetic field configurations or a decreasing external pressure help provide for stabilisation.

A third cause relates directly to how the jet is launched. Variations in the jet speed, termed pulsations, will produce internal working surfaces. Even gradual sinusoidal variations will steepen into shock waves as the wave propagates down the jet. Given the knot spacing,  $\Delta D_k$ , and the jet speed  $v_j$ , we estimate the duration between pulses as  $t_k = \Delta D_k/v_j$  which can be written

$$t_k = 1000 \left( \frac{\Delta D_k}{2000 \text{ AU}} \right) \left( \frac{v_j}{100 \text{ km s}^{-1}} \right)^{-1} \text{ yr.} \quad (10.3)$$

This implies that enhanced ejection associated with enhanced accretion provides a natural explanation for jet knots although it is not obvious how velocity variations, rather than jet density variations, result.

There are indications in many outflows that the jet direction is not fixed. There are wiggles in jets, meandering Herbig-Haro flows, widely

spread Herbig-Haro objects and wide-angle outflows. The time scale for these changes can be just tens of years or up to 10,000 years. The change in angle is generally less than  $10^\circ$  although there are examples where it reaches  $40^\circ$ . The cause of the changes in direction is not known. Suggested causes are as follows:

1. The jets' direction follows the spin axis of the accretion disk and the disk is forced to precess by the tidal force of a companion star. Globally, the bipolar flow possesses a point or 'S-symmetry'. The precession time scale is thought to be about 20 times the Keplerian rotation period of the inner collimating disk i.e. it could be a few hundred years. A badly misaligned disk would re-align with the binary orbit in about a precession period due to energy dissipation from tidal shearing.

2. The disk mass is replenished on a timescale of  $M_d/\dot{M}_d$  in the protostellar phases. Or, a merger event between the disk and another condensation may occur. The disk may thus consist of matter with a changing direction of mean spin. Although it depends on the particular source and stage of evolution, the time scale for disk and jet re-orientation probably exceeds 1000 yr.

3. The jet direction into the surrounding cloud is composed of two components: the jet velocity relative to the protostar and the motion of the protostar relative to the cloud. The jet direction is given from the vector sum of these components. If the protostar is part of a very close binary, its velocity component may be comparable to the jet speed and, hence, it produces prominent wiggles in the jet as it orbits. More likely, wiggles of the order of  $1^\circ$  should be quite common. Wide precession would imply a short orbital timescale – of order of years. In addition, a global reflection or 'C-symmetry' is predicted.

4. The accretion disk is warped by radiation from the central star. If the central star provides the power rather than the accretion itself, then the disk is more likely to be unstable to warping. However, warping is much more likely in the outer disk, on scales which do not determine the jet direction.

Each possibility thus has its own peculiarities. Yet, however good our interpretation, we require confirmation which can only really come from resolving the features within the launch region.

## 10.8 Outflow Evolution

### 10.8.1 *The jet flow*

We now gathered together and interpret observations which indicate that evolutionary relationships exist between the protostar, the accretion and the outflow. Here, we quantify these relationships in order to see how a stellar system might be constructed.

The outflowing mass and energy can be estimated through various measurements of the strength of the jets, the outflow and the impact at Herbig-Haro objects. One general method is to constrain the density, temperature and degree of ionisation and so construct a physical model. A second method is to measure the total luminosity from a single emission line and extrapolate using plausible interpretations.

Class 0 molecular jets possess temperatures in the range of 50–200K and mean densities in the range of  $10^4$  to  $10^6$   $\text{cm}^{-3}$ . The high densities are deduced from the properties of CO bullets and intrinsic molecular shocks, which excite  $\text{H}_2$ . Therefore, molecular jets are hypersonic with Mach numbers exceeding 100. They are probably also super-Alfvénic although the magnetic field cannot be tightly and directly constrained. The mass outflow from twin jets of radius  $r_j$  is then  $\dot{M}_{jet} = 2\pi r_j^2 \rho_j v_j$  where the mass density is  $\rho_j$ , assuming a circular cross-section for simplicity. We thus obtain high mass ejection rates:

$$\dot{M}_{jet} = 1.3 \times 10^{-5} \left( \frac{r_j}{500 \text{ AU}} \right)^2 \left( \frac{n_j}{10^5 \text{ cm}^{-3}} \right) \left( \frac{v_j}{100 \text{ km s}^{-1}} \right) M_{\odot} \text{ yr}^{-1}, \quad (10.4)$$

where the hydrogen nucleon density is  $n_j$  and the molecular number density is  $0.5 n_j$  (noting that molecular hydrogen is by far the most abundant molecule).

In contrast, Class II optical jets typically possess high speeds and low densities. The density of electrons is usually derived, and we then require knowledge of the ion level now thought to be only a few per cent. Then, the total density is found to be only  $\sim 10^3$   $\text{cm}^{-3}$  even on the smaller size scale of these atomic jets. The overall result is a much lower mass loss rate:

$$\dot{M}_{jet} = 1.6 \times 10^{-8} \left( \frac{r_j}{100 \text{ AU}} \right)^2 \left( \frac{n_j}{10^3 \text{ cm}^{-3}} \right) \left( \frac{v_j}{300 \text{ km s}^{-1}} \right) M_{\odot} \text{ yr}^{-1}. \quad (10.5)$$

This indicates an evolution in which the mass ejection rate falls as the

accretion rate falls.

Can the supply from the accretion disk supply meet the demands of both jets and the protostar? In §7.8, we found peak mass accretion rates of order  $10^{-5} M_{\odot} \text{ yr}^{-1}$  in Class 0 objects. According to Eq. 9.14, the typical accretion rate for Class II objects is  $\sim 3 \times 10^{-8} M_{\odot} \text{ yr}^{-1}$ . Therefore, very large mass fractions appear to be ejected.

Can these jets supply the bipolar outflows? To prepare an answer, we revise the above jet formulae to provide thrust (momentum flow rates) and powers which can be compared to those derived directly from the outflow observations. The thrust per jet can be written as

$$\dot{F}_{jet} = 5 \times 10^{-4} \left( \frac{\dot{M}_{jet}}{10^{-5} M_{\odot} \text{ yr}^{-1}} \right) \left( \frac{v_j}{100 \text{ km s}^{-1}} \right) M_{\odot} \text{ km s}^{-1} \text{ yr}^{-1} \quad (10.6)$$

and the double jet power is

$$\dot{L}_{jet} = 8.2 \left( \frac{\dot{M}_{jet}}{10^{-5} M_{\odot} \text{ yr}^{-1}} \right) \left( \frac{v_j}{100 \text{ km s}^{-1}} \right)^2 L_{\odot}. \quad (10.7)$$

Note that the predicted jet power from Class 0 protostars is extremely high and is typically of the order of  $0.1\text{--}0.5 L_{bol}$ . We can also now understand how molecules exist in these jets. If the jet contains a standard dust abundance,  $\text{H}_2$  would form very rapidly at the base of a dense jet. Moreover, molecules will be formed particularly efficiently in the denser knots. Even in the absence of dust,  $\text{H}_2$  can re-form in the knots through the  $\text{H}^-$  route discussed in §2.4.3.

### 10.8.2 The bipolar outflow

Three quantities are needed to quantify the energetics of a bipolar outflow. These are the total mass  $M_o$ , half the linear size  $D_o$  and the median outflow velocity  $V_o$ . Then, the kinematic age  $D_o/V_o$  and energy  $(1/2)M_o v_o^2/D_o$  yield the mechanical luminosity of an outflow, defined as  $L_o = (1/2)M_o v_o^3/D_o$ . Similarly, the outflow thrust is defined as  $F_o = M_o v_o^2/D_o$ . It is not obvious how these are related to the present state of the jets and the driving protostar since the mass is that accumulated over the outflow lifetime and the kinematic age may be much smaller than the true age if the jet is precessing.

The bipolar outflow parameters are estimated from the CO emission lines emitted from low rotational levels since these record the accumulating cold mass on assuming some abundance of CO. The results so far obtained

indicate that the thrust and mechanical luminosity increase with the bolometric luminosity of the protostar. The thrust is usually presented since momentum is conserved whatever the interaction, whereas energy is radiated away. Deeply embedded protostars drive outflows with thrust

$$F_{CO} \sim 2 - 10 \times 10^{-5} \left( \frac{L_{bol}}{L_{\odot}} \right)^{0.62} M_{\odot} \text{ km s}^{-1} \text{ yr}^{-1} \quad (10.8)$$

over a broad range of  $L_{bol}$  from 1  $L_{\odot}$  to  $10^6 L_{\odot}$ . Class I outflows are relatively weaker with a relationship

$$F_{CO} \sim 2 - 10 \times 10^{-6} \left( \frac{L_{bol}}{L_{\odot}} \right)^{0.90} M_{\odot} \text{ km s}^{-1} \text{ yr}^{-1}, \quad (10.9)$$

measurable over  $L_{bol}$  from 0.1  $L_{\odot}$  to  $10^2 L_{\odot}$ . Therefore, outflows certainly evolve with protostellar Class but the accretion rate (and hence the final stellar mass) is the most critical factor. This is also apparent in another quite close correlation, between the outflow thrust and the envelope mass (as measured from submillimetre dust emission):-

$$F_{CO} \sim 0.5 - 8 \times 10^{-4} \left( \frac{M_{env}}{M_{\odot}} \right)^{1.2} M_{\odot} \text{ km s}^{-1} \text{ yr}^{-1}. \quad (10.10)$$

We conclude that while accretion declines rapidly, ejection and accretion remain closely coupled as if there is a single mechanism responsible for all protostellar jets. It appears that high-mass fractions are ejected although the actual size of this fraction is difficult to estimate. One feasible scenario takes this fraction to evolve from 0.3–0.5 for Class 0, to 0.1 for Class I and Class II sources.

## 10.9 Impact Theory

Besides the uncertainties concerning the momentum transfer into the jet, getting it out again is also problematic. The standard approach to impacts is based on equating the thrust which reaches the termination shock of the jet to the rate at which stationary external material receives the momentum. The speed at which jet material reaches the termination shock is  $v_j - V_o$ . Therefore, ram pressure balance yields

$$\rho_j A_j (v_j - V_o)^2 = \rho_c A_c V_o^2. \quad (10.11)$$

where the effective areas of impact,  $A_j$  and  $A_c$ , in the jet and cloud may differ. We shall put  $\eta = \rho_j/\rho_c$  as the ratio of jet density to cloud density.

For heavy or ballistic jets,  $\eta > 1$  and  $v_j \sim v_o$ , which means that the termination shock simply brushes aside the cloud and only a small fraction of the jet momentum will reach the external medium. If ballistic jets are associated with Class 0 outflows, then it would not be easy to understand the high mechanical thrust and luminosity. Furthermore, the bow shock should be the brighter shock due to the high speed but the weaker jet shock may show up as a non-dissociative shock i.e. a molecular knot.

On the other hand, if the jet is light, then the momentum is efficiently transferred but most of the energy remains within the cavity created by the shocked jet material. To determine the most favourable transfer conditions we write the thrust and power transferred at the impact as

$$F_{impact} = \rho_c A_c V_o^2 = \left(1 - \frac{V_o}{V_j}\right)^2 F_{jet} \quad (10.12)$$

and

$$L_{impact} = 0.5 \rho_c A_c V_o^3 = \left(\frac{V_o}{V_j}\right) \left(1 - \frac{V_o}{V_j}\right)^2 L_{jet}. \quad (10.13)$$

Then, it can be shown that the maximum power ratio is  $L_{impact}/L_{jet} = 4/27$ , occurring if  $V_o = V_j/3$  (and  $\eta = 1/4$  if the areas are equal).

The observations suggest that the momentum transfer is probably more efficient than standard theory predicts. Higher efficiency may be achieved through precession which will better distribute the momentum of a heavy jet. In addition, the outflow age may then exceed the kinematic age, relaxing the demand on momentum placed by the simple models.

## 10.10 Summary

Outflow phenomena contain a fossil record of the accretion process, and the further study of bipolar outflows is expected to shed light on the star formation process itself. Outflows are thought to remove excess angular momentum from the accretion disks and to regulate the stellar rotation so that stars continue to grow without spinning up to break-up speeds. Most attractive in these respects is the X-wind model which combines a disk wind, driven by magnetic and centrifugal forces, with disk accretion via mass transfer to a stellar magnetosphere. MHD models can extract the

angular momentum along with 10–30% of the disk mass. Such high mass loss rates are necessary to explain the power of molecular jets and outflows.

The impact of the jets and outflows could be critical to the star formation process. By feeding turbulence back into the core, and raising the sound speed, the outflow might temporarily speed up the accretion. If the bipolar outflow disrupts the cloud, however, then the accretion will subsequently be cut off. Finally, jet impact onto neighbouring cores could also trigger collapse in them. In regions containing many cores, sequential star formation could result.

